Index Modulation Aided Fragmented Spectra Centralization in OTFS Systems

Bo Zhang, *Graduate Student Member, IEEE*, Lin Mei, *Member, IEEE*, Zhaopeng Du, *Graduate Student Member, IEEE*, Kah Chan Teh, *Senior Member, IEEE*, and Ertugrul Basar, *Fellow, IEEE*

***Abstract*—By selecting various active-silent combinations, classical frequency-domain index modulation (IM) generates numerous energy-free subcarriers dispersed across subblocks, which we refer to as the fragmented spectra. This letter proposes a novel IM approach aimed at collecting the fragmented spectra in subblocks to form a completely unused frequency band, called the IM-aided fragmented spectra centralization (IM-FSC). Specifically, within each subblock, if the last subcarrier is to be activated, we transfer this active position to the first unactivated subcarrier and employ a distinguishable constellation to modulate the symbol on this subcarrier. Through this approach, each subblock contributes one energy-free subcarrier, and the unused frequency band can be obtained accordingly by combining these fragmented spectra from multiple subblocks. We designate this unoccupied frequency band as zero padding (ZP) and guard interval for interference cancellation and channel estimation in orthogonal time frequency space (OTFS) system. The closed-form expressions of bit error rate (BER) and generalization guidelines are also derived. Simulation results demonstrate the promising communication capability and channel estimation accuracy of the proposed scheme.**

***Index Terms*—Index modulation (IM), OTFS, fragmented spectra centralization, BER, channel estimation.**

I. Introduction

THE EVOLUTION of sixth generation (6G) is in full swing, envisioned as a paradigm shift aiming to integrate multiple functions, including sensing, communication, control, and radar [1], [2]. In the development process of wireless communication, a persistent paradox emerges: the increasing demands for speed, capacity, energy consumption, and coverage with the scarce communication resources, highlighting the paramount significance of spectral utilization.

Manuscript received 26 March 2024; accepted 25 April 2024. Date of publication 2 May 2024; date of current version 11 July 2024. This work was supported in part by the Natural Science Foundation of China under Grant 62201307, and in part by the Major Key Project of Peng Cheng Laboratory under Grant PCL2024A01. The associate editor coordinating the review of this article and approving it for publication was Y. Fu. *(Corresponding author: Lin Mei.)*

Bo Zhang and Zhaopeng Du are with the School of Electronics and Information Engineering, Harbin Institute of Technology, Harbin 150001, China (e-mail: bozhang@stu.hit.edu.cn; duzhaopeng@stu.hit.edu.cn).

Lin Mei is with the School of Electronics and Information Engineering, Harbin Institute of Technology, Harbin 150001, China, and also with the Department of Broadband Communications, Peng Cheng Laboratory, Shenzhen 518055, China (e-mail: meilin@hit.edu.cn).

Kah Chan Teh is with the School of Electrical and Electronic Engineering, Nanyang Technological University, Singapore 639798 (e-mail: ekcteh@ntu.edu.sg).

Ertugrul Basar is with the Department of Electrical and Electronics Engineering, Koç University, 34450 Istanbul, Turkey (e-mail: ebasar@ku.edu.tr).

Digital Object Identifier 10.1109/LWC.2024.3396278

Over the past decade, index modulation (IM) [3] has been considered as a highly spectrum-efficient technology, which only activates a subset of available transmission entities (such as subcarriers, antennas, and time slots). By selecting various patterns of the "active-silent" transmission entities during transmission process, additional bits can be conveyed implicitly, thereby enhancing the spectral efficiency (SE) [4]. This allows the IM-based technologies to achieve the same throughput as their conventional counterparts while utilizing only a fraction of the resources, thus consuming less energy.

However, it is precisely due to the partially activated characteristic that a large amount of energy-free subcarriers would appear in most frequency-domain IM systems, which we refer to as the fragmented spectra. To fully exploit the fragmented spectra, several IM variants have been proposed [5], [6], [7]. In [5], another distinguishable constellation has been employed on the subcarriers intended to remain silent, which improves the SE. Multiple-mode IM proposed in [6] adopts the permutations of multiple distinguishable signal constellations instead of the combinations of active-silent statuses. In [7], cascaded IM has been performed, which preserves silent subcarriers while employing two distinguishable constellations within a subblock, leading to an increase in the number of index bits. However, little attention has been paid to integrating the fragmented spectra into a relatively wide, unoccupied frequency band.

Against this background, this letter presents a novel *IM aided fragmented spectra centralization (IM-FSC)* scheme to enhance the spectral utilization. Specifically, within each subblock, activating the last subcarrier would lead a transfer of this active position to the first silent subcarrier. A distinguishable constellation is then employed to modulate the symbol on this subcarrier. Through this approach, each subblock could offer one energy-free subcarrier. By integrating fragmented spectra across multiple subblocks, the unused frequency band can be obtained. We attempt to use this frequency band as guard null symbols or zero padding (ZP) for the orthogonal time frequency space (OTFS) system [8]. Channel estimation in OTFS [9] is also considered to be carried out in this frequency band, as it requires a large number of guard symbols between data and pilot. The closed-form upper bound expressions of bit error rate (BER) are also derived, alongside insights for potential generalization of the IM-FSC scheme.

Notation: $\mathbf{F}_M$ denotes the normalized M-point fast Fourier transform (FFT) matrix. C_a^b represents the number of ways to choose b elements from a set of size a. $\otimes$ represents the Kronecker product. $\mathbf{A}[i, j]$ denotes the entries (i, j) of matrix $\mathbf{A}$. diag$\{\mathbf{a}\}$ denotes the diagonal matrix created by vector $\mathbf{a}$.

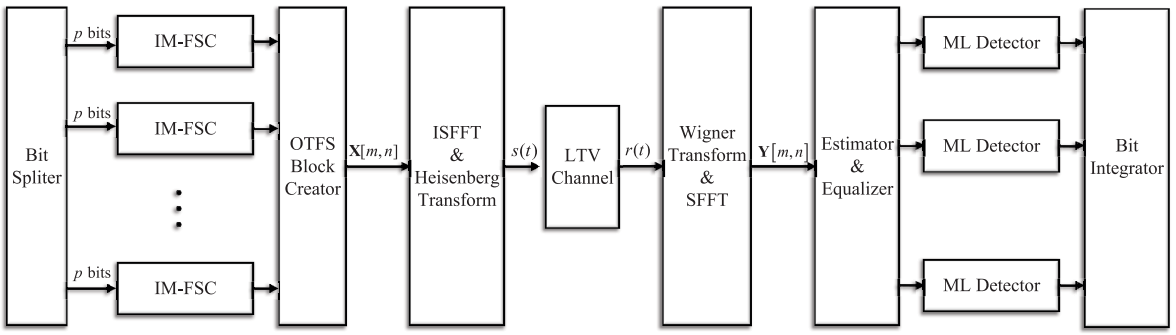

Fig. 1. The block diagram of the IM-FSC scheme for OTFS.

II. System Model

At the OTFS transmitter, MN modulated symbols are placed on the $M \times N$ grid in the delay-Doppler (DD) domain, where M and N denote the number of subcarriers and time slots, respectively. The subcarrier spacing and time slot duration are denoted by Δf and T.

A. IM-FSC

The block diagram of OTFS with IM-FSC (OTFS-IM-FSC) system is presented in Fig. 1. In the context of IM, the MN grid points in the DD domain are initially divided into g subblocks, each containing $a = MN/g$ grid points. Assume that b of a grid points in a subblock are available for activation with $b < a$. The p bits transmitted in each subblock are separated into two parts with $p = p_1 + p_2$. p_1 bits are used to generate the active index set, denoted as $\theta = \{\alpha_1, \alpha_2, \ldots, \alpha_b\}$, where $\alpha_e \in \{1, 2, \ldots, a\}$ for $e = 1, 2, \ldots, b$, and p_2 bits are utilized to generate the modulated symbols from $\mathcal{M}$-ary constellation alphabet $\mathbb{S}_A$. The rest grid points in the subblock are considered as the silent indices, which are expressed as $\vartheta = \{\beta_1, \beta_2, \ldots, \beta_{a-b}\}$ with $\vartheta \cap \theta = \varnothing$. Assume that the elements in θ and ϑ are arranged in ascending order. In the IM-FSC scheme, the last active index α_b in θ will be checked according to the following criteria. If $\alpha_b = a$, indicating that the last grid point in subblock is to be activated, α_b will be replaced by the first silent index in ϑ, i.e., β_1, and then the distinguishable $\mathcal{M}$-ary alphabet $\mathbb{S}_B$ is utilized to modulate the symbol on β_1. Through the IM-FSC scheme, each subblock can contribute one energy-free grid point. By collecting all the fragmented spectra in subblocks, the unused frequency band can be created. Fig. 2 shows the working process of the IM-FSC scheme in OTFS system, where subblocks in the two-dimensional (2D) $M \times N$ grid are vertically distributed. The classic theory of designing $\mathbb{S}_A$ and $\mathbb{S}_B$ has been discussed in detail in [5] and [6] with the principle of maximizing the minimum distance between $\mathbb{S}_A$ and $\mathbb{S}_B$. Under the average power constraint, $\mathcal{M}$-ary constellation points are considered to be uniformly distributed on a power-normalized circle as $\mathcal{M}$ goes infinity. Taking the phase shift keying (PSK) as an example, for the $\mathcal{M}$-ary constellation alphabet $\mathbb{S}_A$, $\mathbb{S}_B$ could be obtained by rotating the angle of $\pi/\mathcal{M}$ by $\mathbb{S}_A$.

In this letter, the centralized frequency band serves as ZP, forming the ZP-OTFS [8] system. Assuming that the OTFS system requires a ZP of length L_{zp}, the IM-FSC scheme could meet this requirement with $N \times L_{zp}$ subblocks, transmitting a total of pNL_{zp} bits. The SE could be expressed as $\frac{pNL_{zp}}{aNL_{zp}} = \frac{p}{a}$, whereas the SE of IM scheme is $\frac{p}{a+1}$ while maintaining the same ZP and transmitted bits.

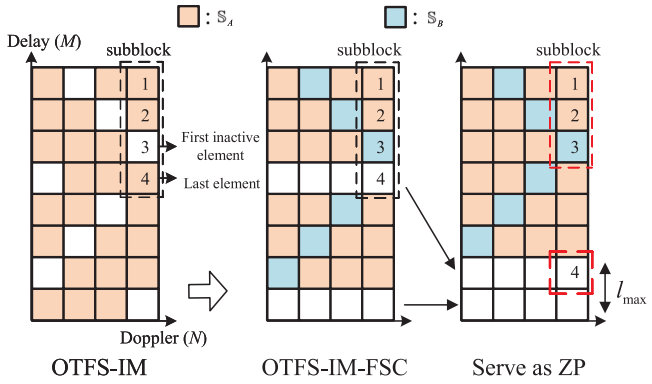

Fig. 2. The working process of IM-FSC in OTFS systems for $M = 8$, $N = 4$, $a = 4$, and $b = 3$.

B. Prospects for Generalization of IM-FSC

The fundamental challenge in all IM-based systems lies in finding communication resources that are orthogonal or minimally impacting on each other to label transmission entities, thereby distinguishing different transmission patterns. The optimal communication resources for labeling should be perfectly orthogonal, such as transmission on the real and imaginary parts, while suboptimal resources should exhibit limited mutual interference, such as distinguishable constellations. The technical challenge of the proposed IM-FSC scheme also revolves around this aspect.

It should be noted that the purpose of this letter is not to propose the IM-FSC method that only uses distinguishable constellations to label the transmission entities, but to illustrate the concept of centralizing fragmented spectra through the example of distinguishable constellations $\mathbb{S}_A$ and $\mathbb{S}_B$. It is definitely possible to use different time slots, antennas, or other entities to replace $\mathbb{S}_A$ and $\mathbb{S}_B$ for the IM-FSC process. The centralized spectra can support various applications, including ZP, sensing, radar, etc. Discovering optimal labeling entitles holds the potential to significantly enhance the performance of

IM-FSC and expand its applicability across various systems. Considering that multiple orthogonal modes are available in the orbital angular momentum (OAM), applying it to IM-FSC would be an ideal choice for future research. Additionally, this letter primarily discusses the selection of distinguishable PSK constellations. According to the conclusions in [6], the usage of distinguishable quadrature amplitude modulations (QAM) is more favorable for $\mathcal{M} > 4$. Due to the fact that rotating BPSK by $\pi/2$ leads to the non-interfering constellations, it is always recommended in the IM-FSC scheme.

C. Input-Output Relations

Theoretically, the centralized frequency band holds flexibility regarding its position on the 2D $M \times N$ grid. In this letter, the centralized frequency band is used as ZP to mitigate interference. Due to the need for numerous guard null symbols for OTFS channel estimation, the pilot is also inserted into this frequency band to enhance resource utilization. Once the delay-Doppler signal $\mathbf{X} \in \mathbb{C}^{M\times N}$ is settled, the 2D time-domain signal can be derived through the inverse symplectic Fourier transform (ISFFT) and Heisenberg transform with pulse-shaping waveform $\mathbf{G}_{\text{tx}}$ as

$$\mathbf{S} = \mathbf{G}_{\text{tx}}\mathbf{F}_M^H\left(\mathbf{F}_M\mathbf{X}\mathbf{F}_N^H\right) = \mathbf{G}_{\text{tx}}\mathbf{X}\mathbf{F}_N^H. \tag{1}$$

After column-wise vectorization of $\mathbf{S}$, the time-domain signal $s(t)$ is transmitted through the time-varying channel with channel response $h(\tau,\nu)$, given as

$$\begin{aligned} r(t) &= \iint h(\tau,\nu)s(t-\tau)e^{j2\pi v(t-\tau)}d\tau d\nu + \omega(t) \\ &= \int \mathrm{g}(\tau,t)\ s(t-\tau)d\tau + \omega(t), \end{aligned} \tag{2}$$

where P, τ, ν, and $\omega(t)$ denote the distinguishable path number, delay, Doppler shift, and zero mean Gaussian noise, respectively. The discrete signal at the receiver is obtained by sampling $r(t)$ at $t = qT_s = qT/M$ as

$$r[q] = \sum_l \mathrm{g}^{\mathrm{s}}[l,q]\ s[q-l] + \omega(q),\ \ q = 0,\ldots,NM-1, \tag{3}$$

where $l = \tau/T_s$. (3) could also be expressed in matrix form as $\mathbf{r} = \mathbf{G}\mathbf{s} + \mathbf{w} \in \mathbb{C}^{MN\times 1}$, where $\mathbf{G} \in \mathbb{C}^{MN\times MN}$. Considering a time-varying channel with P paths, where the normalized delay l_i and Doppler shift k_i for i-th path are assumed to be integers, $\mathrm{g}^{\mathrm{s}}[l,q]$ could be simplified as

$$\mathrm{g}^{\mathrm{s}}[l,q] = \sum_{i=1}^{P} h_i z^{k_i(q-l)}\delta[l-l_i], \tag{4}$$

where $z = \frac{j2\pi}{MN}$ and h_i denotes the channel gain for i-th path.

After converting the received signal vector $\mathbf{r}$ into the $M \times N$ matrix $\mathbf{R}$, Wigner transform with pulse-shaping waveform $\mathbf{G}_{\text{tx}}$ and SFFT are employed successively to obtain the DD-domain signal $\mathbf{Y} = \mathbf{F}_M^H(\mathbf{F}_M\mathbf{G}_{\text{rx}}\mathbf{R})\mathbf{F}_N$. For brevity, the rectangular pulses are assumed, i.e., $\mathbf{G}_{\text{tx}} = \mathbf{G}_{\text{rx}} = \mathbf{I}_M$. After the column-wise vectorization of $\mathbf{Y}$, we could get

$$\mathbf{y} = \underbrace{(\mathbf{F}_N \otimes \mathbf{I}_{\mathrm{M}})\mathbf{G}\left(\mathbf{F}_M^H \otimes \mathbf{I}_{\mathrm{M}}\right)}_{\mathbf{H}_{\text{eff}}}\mathbf{x} + \underbrace{(\mathbf{F}_N \otimes \mathbf{I}_{\mathrm{M}})\mathbf{w}}_{\mathbf{z}}, \tag{5}$$

where $\mathbf{H}_{\text{eff}} \in \mathbb{C}^{MN\times MN}$ and $\mathbf{z} \in \mathbb{C}^{MN\times 1}$ denote the effective channel matrix in the DD domain and the additive noise samples vector with $\mathcal{CN}(0,N_0)$, respectively.

Since each vertically distributed subblock can contribute one energy-free subcarrier in the OTFS-IM-FSC system, there will be a $\frac{M}{a} \times N$ grid served as ZP. Pilot symbol is also placed in this grid to improve the resource utilization. Let l_{max} and k_{max} denote the maximum delay and Doppler taps. Assuming the location of pilot symbol x_p is $\mathbf{X}[m_p,n_p]$. According to [9], the protection interval between data symbols $x_d[m,n]$ and pilot should be set to at least $2l_{max} \times 4k_{max}$, which requires $M \geq 2al_{max}$ and $N \geq 4k_{max}$. It is reasonable to place the pilot in the center of the $\frac{M}{a} \times N$ energy-free grid, i.e., m_p and n_p should be around $\frac{M}{2a}$ and $N/2$, respectively. The embedded-pilot signal in the DD domain could be expressed as

$$\mathbf{X}[m,n] = \begin{cases} x_p & m = m_p, n = n_p, \\ x_d[m,n] & 1 \leq m \leq \frac{M(a-1)}{a}, \\ 0 & \text{otherwise}, \end{cases} \tag{6}$$

which is called *embedded-pilot with full guard symbols* in [9]. By omitting the effect of noise, the input-output relationship in DD domain can also be written as [10]

$$\begin{aligned} \mathbf{Y}\left[m_p+l_i, n_p+k_i\right] &= h[l_i,k_i]z^{k_i m_p}\mathbf{X}\left[m_p,n_p\right] \\ &= h_i z^{k_i m_p}x_p, \end{aligned} \tag{7}$$

where the subscript i stands for the i-th path for $i = 1,\ldots,P$. By setting a threshold $\mathcal{T}$ to determine whether the path with delay l and Doppler k exists, the channel parameters (l, k) could be estimated as

$$t[l,k] = \begin{cases} 1 & \left|\mathbf{Y}\left[m_p+l, n_p+k\right]\right| \geq \mathcal{T}, \\ 0 & \text{otherwise}, \end{cases} \tag{8}$$

where the path number is estimated by $\check{P} = \sum_l\sum_k t[l,k]$. With the estimated delay and Doppler, the channel gain can be derived through (7). Given the channel parameters $(\check{P}, l, k, h[l,k])$, the channel matrix can be rebuilt.

D. Detector

The index detector is used after the channel estimator and equalizer to recover transmitted bits. The maximum likelihood (ML) detector considers all possible active patterns in each subblock and makes joint decisions on the indices and information symbols, achieving optimal performance. This process can be expressed using mathematical formula as

$$\left(\hat{\theta},\hat{\mathcal{S}}\right) = \underset{\alpha_\xi\in\theta,\mathcal{S}\in\{\mathbb{S}_A,\mathbb{S}_B\}}{\arg\min} \sum_{\xi=1}^{b}\left|y\left(\alpha_\xi\right) - \mathcal{S}(\xi)\right|^2. \tag{9}$$

III. Performance Analysis

A. BER

The BER of the OTFS-IM-FSC system can be derived by considering two cases: the indices are erroneously detected, which results in a BER of approximately 0.5; the indices are correctly detected, but the symbols are incorrectly determined. The BER expressions are derived in the flat Rayleigh fading channel, which models the multipath fading

without direct line-of-sight (LOS) paths. The index error probability is analyzed at first. Recalling (5) with $\mathbf{H}_{\text{eff}} = \text{diag}\{h(1), \ldots, h(MN)\}$, the following cases are investigated to obtain the BER of indices under ML detector: the erroneous detection of constellation $\mathbb{S}_B$ as $\mathbb{S}_A$ on index β_1, denoted as $P_{r1}(\mathbb{S}_B \to \mathbb{S}_A)$; the misjudgment of active index α as a silent index $\tilde{\alpha}$, denoted as $P_{r2}(\alpha \to \tilde{\alpha})$. The conditional pairwise error probability (CPEP) of P_{r1} can be expressed as

$$\begin{aligned} P_{r1}(\mathbb{S}_B \to \mathbb{S}_A) &= P_{r1}\Big\{|y(\beta_1) - \mathcal{S}_B(\beta_1)h(\beta_1)|^2 \\ &\quad > |y(\beta_1) - \mathcal{S}_A(\beta_1)h(\beta_1)|^2\Big\} \\ &= P_{r1}\Big\{\mathfrak{Re}\{h(\beta_1)z(\beta_1)[\mathcal{S}_A(\beta_1) - \mathcal{S}_B(\beta_1)]\} \\ &\quad > \frac{1}{2}|\mathcal{S}_B(\beta_1) - \mathcal{S}_A(\beta_1)|^2|h(\beta_1)|^2\Big\}. \quad (10) \end{aligned}$$

It is worth noting that $|\mathcal{S}_B(\beta_1) - \mathcal{S}_A(\beta_1)|$ actually denotes the minimum distance between $\mathbb{S}_B$ and $\mathbb{S}_A$, which equals to $2\sin\frac{\pi}{2\mathcal{M}}\sqrt{\varphi E_s}$ for PSK constellation, and $\mathfrak{Re}\{h(\beta_1)z(\beta_1)[\mathcal{S}_A(\beta_1) - \mathcal{S}_B(\beta_1)]\}$ is Gaussian distributed with $\mathcal{N}(0, 2\varphi E_s N_0|h(\beta_1)|^2)$, where φ and E_s are the power scaling factor and symbol power, respectively. Since the SE of the IM-FSC scheme has been improved by $1/a$ compared to the IM scheme, φ equals to $\frac{a}{b}$ and $\frac{a+1}{b}$ in the IM and IM-FSC schemes, respectively. After some algebraic computations [11], (10) could be expressed as

$$\begin{aligned} P_{r1}(\mathbb{S}_B \to \mathbb{S}_A) &= Q\left(\frac{2\sin^2\frac{\pi}{2\mathcal{M}}\varphi E_s|h(\beta_1)|^2}{\sqrt{2\varphi E_s N_0|h(\beta_1)|^2}}\right) \\ &= Q\Big(\sin^2\frac{\pi}{2\mathcal{M}}\sqrt{2\overline{\gamma}v_\beta}\Big), \end{aligned} \quad (11)$$

where $\overline{\gamma} = \frac{\varphi E_s}{N_0}$ denotes the average signal to noise ratio (SNR) and $v_\beta = |h(\beta_1)|^2$. By approximating the Q function with $Q(x) \approx \frac{1}{12}\mathrm{e}^{-x^2/2} + \frac{1}{4}\mathrm{e}^{-2x^2/3}$ and applying the well-known moment generating function (MGF), (11) could be simplified as

$$P_{r1}(\mathbb{S}_B \to \mathbb{S}_A) \approx \frac{1}{12}\Big(1 + d^4\overline{\gamma}\Big)^{-1} + \frac{1}{4}\left(1 + \frac{4d^4\overline{\gamma}}{3}\right)^{-1}, \quad (12)$$

where $d = \sin\frac{\pi}{2\mathcal{M}}$. Following the steps from (10) to (12), P_{r2} can also be derived as

$$\begin{aligned} P_{r2}(\alpha \to \tilde{\alpha}) &= P_r\Big\{|y(\alpha) - x(\alpha)h(\alpha)|^2 + |y(\tilde{\alpha})|^2 \\ &\quad > |y(\alpha)|^2 + |y(\tilde{\alpha}) - x(\alpha)h(\tilde{\alpha})|^2\Big\} \\ &\approx \frac{1}{12}\left[\left(1 + \frac{\overline{\gamma}}{8}\right)^{-2} + 3\left(1 + \frac{\overline{\gamma}}{6}\right)^{-2}\right], \end{aligned} \quad (13)$$

where $y(\alpha) = x(\alpha)h(\alpha) + z(\alpha)$ and $y(\tilde{\alpha}) = z(\tilde{\alpha})$. Assuming equal activation probability for each subcarrier within the subblock and considering the proportion of two cases, the instantaneous index error probability can be expressed as $P_r(\alpha \to \check{\alpha}) = \frac{1}{a}P_{r1}(\mathbb{S}_B \to \mathbb{S}_A) + \frac{a-1}{a}P_{r2}(\alpha \to \tilde{\alpha})$, where $\check{\alpha}$ denotes the misjudged index. The average index error probability can then be achieved by using the union bound as

$$\overline{P}_I = \frac{b}{a}\sum_{\alpha=1}^{a}\sum_{\check{\alpha}\neq\alpha=1}^{a-b} P_r(\alpha \to \check{\alpha}). \quad (14)$$

The well-known average symbol error probability of $\mathcal{M}$-ary PSK [12] is given as

$$\overline{P}_{\mathcal{M}} \approx \frac{\varsigma}{12}\left[\frac{1}{1 + \bar{\gamma}\rho} + \frac{9}{3 + 4\bar{\gamma}\rho}\right], \quad (15)$$

where $\rho = \sin\frac{\pi}{\mathcal{M}}$ and $\varsigma = 1, 2$ for $\mathcal{M} = 2$ and $\mathcal{M} > 2$, respectively. The closed-form upper bound expression of BER for the IM-FSC scheme can be derived as

$$P_b \le \left(\overline{P}_I\frac{p_1 + p_2}{2} + \frac{\overline{P}_{2\mathcal{M}}}{\log_2\mathcal{M}}(1 - \overline{P}_I)p_2\right)(p_1 + p_2)^{-1}, \quad (16)$$

where $p_1 = \lfloor\log_2 C_a^b\rfloor$ and $p_2 = b\log_2\mathcal{M}$.

IV. Numerical Results and Discussion

In this section, Monte Carlo simulations are conducted to evaluate the performance of the OTFS-IM-FSC system. The wireless channel characteristics are modeled based on the 3GPP vehicular channel models, specifically employing the extended vehicular A (EVA) model, featuring delays [0, 0.03, 0.15, 0.31, 0.37, 0.71, 1.09, 1.73, 2.51] (μs) and corresponding relative powers [0, −1.5, −1.4, −3.6, −0.6, −9.1, −7.0, −12.0, −16.9] (dB). The user speed and carrier frequency are set to 500 km/h and 4 GHz. Doppler shifts are generated following a uniform distribution $U(0, \nu_{max})$, where ν_{max} denotes the maximum Doppler shift. For the OTFS parameters, we choose $M = 64$, $N = 16$, and Δf=15 kHz. E_b/N_0 is utilized to assess the quality of the received signal, where E_b represents the energy per bit. The pilot SNR is defined as $\text{SNR}_p = |x_p|^2/N_0$, and the threshold $\mathcal{T}$ is set to $3\sqrt{1/\text{SNR}_p}$ according to [9]. We also refer "OTFS-IM-FSC $(a, b, \mathcal{M})$" as the OTFS-IM-FSC system with b out of a elements activated in each subblock, transmitting the $\mathcal{M}$-ary symbols.

In Fig. 3, the BER comparison is presented between the theoretical and simulated curves for the OTFS-IM-FSC system. It can be observed that as the SNR increases, the simulated curve gradually converges towards the theoretical upper bound (16). Specifically, when the SNR exceeds 25 dB (BER $< 10^{-3}$), two curves begin to align. When SNR $>$ 30 dB, the simulated results are precisely matched with the derived theoretical performance, affirming the reliability of our previous analysis.

In Fig. 4, the normalized mean square error (NMSE) between the estimated channel matrix and the perfect channel matrix is presented by varying SNR_p. It can be seen that as SNR_p increases, the estimated channel gradually converges towards the perfect channel. However, there is an error floor in the SNR range of 30-40 dB, which is mainly related to the threshold $\mathcal{T}$ in (8). Setting a small $\mathcal{T}$ may lead to inaccurate channel estimation, where noise and interference could be incorrectly estimated as part of the channel. Conversely, increasing the threshold beyond a certain value may result in

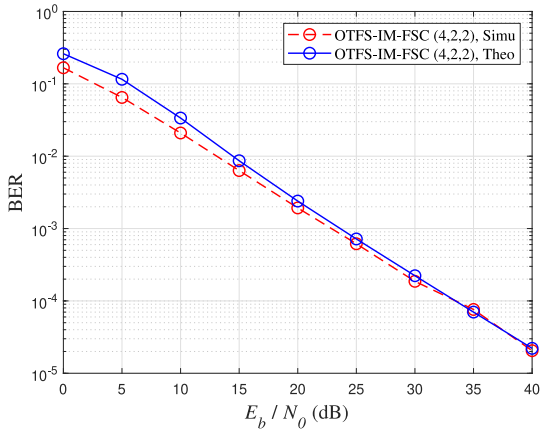

Fig. 3. The theoretical and simulated BER performance of OTFS-IM-FSC system using ML detector.

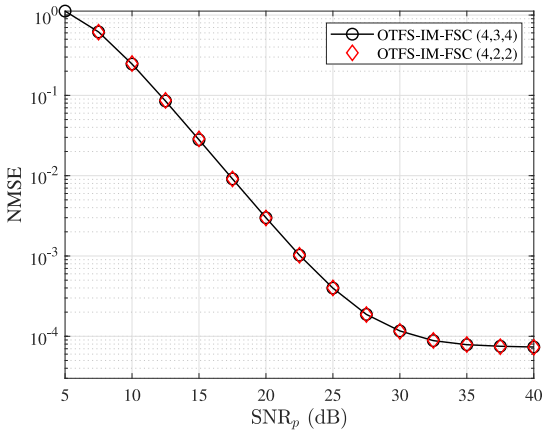

Fig. 4. The NMSE between the estimated channel matrix and the perfect channel matrix in delay-Doppler domain.

incomplete channel estimation, where paths with lower power are ignored. The EVA channel contains certain paths with extremely low power (-16.9 dB), which can not be accurately estimated under a fixed threshold $\mathcal{T} = 3\sqrt{1/\mathrm{SNR}_p}$. The optimal threshold that balances the probabilities of false detection and missed detection can be obtained by progressively adjusting $\mathcal{T}$ in different SNR_p regions. In addition, due to sufficient protection interval in the OTFS-IM-FSC system, the transmitted data does not affect the results of channel estimation.

Fig. 5 shows the comparison of BER between the OTFS-IM-FSC and OTFS-IM systems with $\mathrm{SNR}_p = 40$ dB. The classical minimum mean squared error (MMSE) and maximum ratio combining Gauss-Seidel (MRC-GS) [8] algorithms are utilized to equalize the channel. All parameters are carefully selected to achieve the same SE for all compared schemes. From Fig. 5, it is evident that the BER curves using estimated channel closely align with the curves derived from perfect channel knowledge. Furthermore, the OTFS-IM-FSC system outperforms the OTFS-IM system under the same receiver and SE, with a gain of approximately 1.67 dB at BER of 10^{-3} for parameter sets (2,1,2) and (4,3,2). This improvement can be attributed to the enhanced SE of the OTFS-IM-FSC system, resulting from increased spectral utilization.

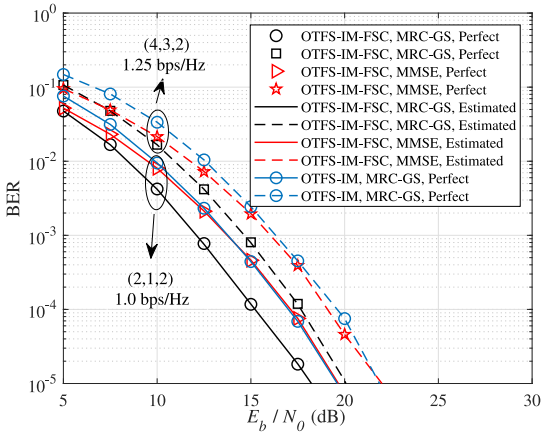

Fig. 5. Performance comparison between the OTFS-IM-FSC and OTFS-IM systems with different parameters.

V. Conclusion

The pursuit for high spectral utilization schemes in wireless communication demands a paradigm shift towards innovative approaches. This letter proposes the IM-FSC scheme to enhance spectral utilization. By centralizing the fragmented spectra, IM-FSC offers a unique solution for interference cancellation and channel estimation in OTFS systems. The essence of IM-FSC is the concept of centralizing fragmented resources, providing a blueprint for efficient resource allocation. Through this approach (illustrated using distinguishable constellations), not only fragmented spectra, other fragmented resources like fragmented time slots can also be centralized in a similar way. The prospects for potential generalization of the IM-FSC scheme are also discussed in this letter, offering insights for future research.

References

[1] K. B. Letaief, Y. Shi, J. Lu, and J. Lu, "Edge artificial intelligence for 6G: Vision, enabling technologies, and applications," *IEEE J. Sel. Areas Commun.*, vol. 40, no. 1, pp. 5–36, Jan. 2022.

[2] W. Saad, M. Bennis, and M. Chen, "A vision of 6G wireless systems: Applications, trends, technologies, and open research problems," *IEEE Netw.*, vol. 34, no. 3, pp. 134–142, May/Jun. 2020.

[3] S. Doğan Tusha, A. Tusha, E. Basar, and H. Arslan, "Multidimensional index modulation for 5G and beyond wireless networks," *Proc. IEEE*, vol. 109, no. 2, pp. 170–199, Feb. 2021.

[4] E. Basar, U. Aygölü, E. Panaylrcl, and H. V. Poor, "Orthogonal frequency division multiplexing with index modulation," *IEEE Trans. Signal Process.*, vol. 61, no. 22, pp. 5536–5549, Nov. 2013.

[5] T. Mao, Z. Wang, Q. Wang, S. Chen, and L. Hanzo, "Dual-mode index modulation aided OFDM," *IEEE Access*, vol. 5, pp. 50–60, 2017.

[6] M. Wen, E. Basar, Q. Li, B. Zheng, and M. Zhang, "Multiple-mode orthogonal frequency division multiplexing with index modulation," *IEEE Trans. Commun.*, vol. 65, no. 9, pp. 3892–3906, Sep. 2017.

[7] T. Mao, Q. Wang, J. Quan, and Z. Wang, "Zero-padded tri-mode index modulation aided OFDM," in *Proc. IEEE Global Commun. Conf. (GLOBECOM)*, 2017, pp. 1–5.

[8] T. Thaj and E. Viterbo, "Low complexity iterative rake decision feedback equalizer for zero-padded OTFS systems," *IEEE Trans. Veh. Technol.*, vol. 69, no. 12, pp. 15606–15622, Dec. 2020.

[9] P. Raviteja, K. T. Phan, and Y. Hong, "Embedded pilot-aided channel estimation for OTFS in delay-doppler channels," *IEEE Trans. Veh. Technol.*, vol. 68, no. 5, pp. 4906–4917, May 2019.

[10] Y. Hong, T. Thaj, and E. Viterbo, *Delay-Doppler Communications: Principles and Applications*. Amsterdam, The Netherlands: Elsevier, 2022.

[11] M. Simon and M. Alouini, *Digital Communication Over Fading Channels*. Hoboken, NJ, USA: Wiley, 2005.

[12] J. G. Proakis, *Digital Communications*. New York, NY, USA: McGraw-Hill, 2008.